Supplementary Information

A far-red fluorescent probe for sensing laccase in fungi and its application to develop an effective biocatalyst for biosynthesis of antituberculous dicoumarin

Zhenhao Tian,[a,b‡] Qingsong Yan,[a‡] Lei Feng,[a,b‡] Sa Deng,[a] Chao Wang,[*,a,b] Jingnan Cui,[b] Chunjie Wang,[a] Zhanjun Zhang,[d] Tony D. James,[*,c] and Xiaochi Ma[*,a]

[a.] National-Local Joint Engineering Research Center for Drug–Research and Development of Neurodegenerative Disease, Academy of Integrative Medicine, College of Pharmacy, Dalian Medical University, Dalian 116044, China.
E-mail: wach_edu@sina.com (C. Wang), maxc1978@163.com (X.C. Ma)

[b.] State Key Laboratory of Fine Chemicals, Dalian University of Technology, Dalian 116024, China.

[c.] Department of Chemistry, University of Bath, Bath BA2 7AY, United Kingdom.
E-mail: t.d.james@bath.ac.uk (T.D. James)

[d.] State Key Laboratory of Cognitive Neuroscience and Learning, Beijing Normal University, Beijing, China.

[‡] These authors contributed equally to this work.

Index

Experimental section

Materials and instruments

All of the chemical reagents and solvents were obtained from Tianjin Kemiou Chemical Reagent Co., Ltd. (Tianjin, P.R. China). Laccase (>0.5 U/mg) from *Trametes versicolor* was the product of Shanghai Yuanye Biotech Co., Ltd. (Shanghai, P.R. China). Recombinant CYP1A1, CYP2C19, CYP2D6, CYP2E1, CYP3A4, and CYP3A5 were purchased from Corning Incorporated Life Sciences. Horseradish peroxidase (HRP), tyrosinase (Tyr), lipase, AchE, and BSA were purchased from sigma-aldrich.

NMR spectra were measured using Bruker-600, 500 with tetramethylsilane (TMS) as the internal standard (Bruker, USA). HR-MS data were recorded by an Agilent 1290 infinity 6540 UHD accurate mass Q-TOF MS (Agilent, USA). Fluorescence microscopic imaging was conducted with Leica Confocal Microscope (Leica Microsystems, Germany). The bioassay solutions in 96-well plates were also analyzed using a BioTek Synergy H1 microplate reader (BioTek, USA). The imaging of fungi on plates were recorded in a NightOWL II LB983 small animal *in vivo* imaging system equipped with a sensitive Charge Coupled Device (CCD) camera, with an excitation laser of 630 nm and an emission filter of 650 – 735 nm. HPLC-UV analysis was performed using DIONEX Ultimate 3000 (Thermo Fisher Scientific, USA).

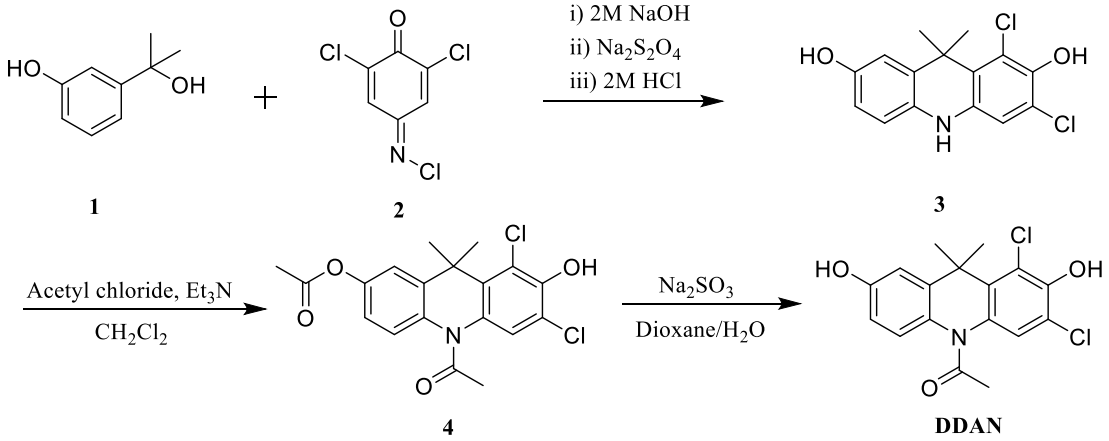

Scheme S1. The synthetic route of **DDAN**.

Synthesis of DDAN

The far-red fluorescent probe **DDAN** was synthesized as shown in Scheme 1.

*Synthesis of compound **3***. 3-(2-hydroxy-2-propyl) phenol (**1**, 1.52 g, 10.0 mmol) and

2,6-dichloroquinone-4-chloroimide (**2**, 2.10 g, 10.0 mmol) were dissolved in 5 mL THF and 5 mL H_2O. Aqueous 2M NaOH (10.5 mL, 21.0 mmol) was added dropwise, and the mixture was stirred for 2 h at 0 ˚C. Then, the reaction solution was poured into 350 mL saturated NH_4Cl aqueous solution, and extracted with 300 mL EtOAc. The organic phase was washed by 10% $Na_2S_2O_4$ aqueous solution and brine. After the evaporation of EtOAc, the residue was dissolved in 10 mL MeOH and then blended into 250 mL deoxygenated aqueous 1M HCl. The resulting suspension was refluxed under an argon atmosphere for 1.5 h. The reacted solution was cooled, extracted twice with EtOAc (200 mL), and the combined extracts washed by brine. Then, the organic phase was dried over anhydrous $MgSO_4$ and concentrated under reduced pressure to afford crude **3**, which was used directly in the next step without further purified.

*Synthesis of compound **4***. To a solution of crude **3** (2.40 g) and triethylamine (4.5 mL) in 50 mL anhydrous CH_2Cl_2, 2.3 mL acetyl chloride was added dropwise and the mixture was stirred for 1 h at room temperature. The resulting solution was washed with water and brine, then dried over anhydrous $MgSO_4$. After the evaporation of solvents, the residue was separated by silica gel column to afford **4** as a white solid (2.01 g). ^{1}H NMR (500 MHz, DMSO-d_6) δ 9.33 (s, 1H), 7.14 (d, J = 2.2 Hz, 1H), 6.90 (s, 1H), 6.83 (dd, J = 8.6, 2.3 Hz, 1H), 6.68 (d, J = 8.6 Hz, 1H), 2.35 (s, 3H), 2.23 (s, 3H), 1.80 (s, 6H). ^{13}C NMR (125 MHz, DMSO-d_6) δ 169.47, 167.99, 144.03, 137.67, 136.04, 132.51, 129.60, 128.16, 125.74, 122.43, 120.65, 120.49, 113.45, 112.79, 37.39, 31.36, 20.79, 19.86. HR-MS (-)-ESI *m/z* 392.0455 $[M-H]^-$ (calcd. 392.0462).

*Synthesis of **DDAN***. To a solution of **4** (393 mg, 1.0 mmol) in 15 mL 1,4-dioxane, 10 mL Na_2SO_3 aqueous solution (1.0 mM) was added dropwise, and the mixture was stirred at 50 ˚C overnight. The resulting solution was diluted with CH_2Cl_2 and washed by water, brine. After removing the solvents, the residue was separated by silica gel column to afford **DDAN** as a white solid (151 mg, 43.1%). ^{1}H NMR (400 MHz, $CDCl_3$) δ 6.82 (s, 1H), 6.61 – 6.51 (m, 2H), 6.41 (d, J = 8.4 Hz, 1H), 5.99 (s, 1H), 4.47 (s, 1H), 2.38 (s, 3H), 1.85 (s, 6H). ^{13}C NMR (125 MHz, MeOD) δ 170.05, 152.26, 139.91, 137.46, 131.77, 129.99, 129.61, 127.52, 123.87, 115.62, 114.94, 114.82, 113.58, 39.15, 32.02, 20.08. HR-MS (-)-ESI *m/z* 350.0349 $[M-H]^-$ (calcd. 350.0356).

Oxidation of DDAN catalyzed by laccase

In the citric acid-phosphate buffer solution (pH 7.4), laccase (1.0 mg/mL) and **DDAN** (10 μM, DMSO < 1%, *v/v*) were co-incubated at 30 ºC for 20 min. Then, acetonitrile (33%, *v/v*) was added to inactivate the laccase activity and terminate the enzymatic reaction. When the denatured proteins were precipitated by centrifugation at 20,000 × *g* for 20 min, the fluorescence intensity corresponding to the production of **DDAO** was measured using Microplate reader with the excitation wavelength at 600 nm and emission wavelength at 658 nm.

Interferences of other species on the fluorescence emission of DDAN and the fluorescence response of DDAN towards laccase

Various ions including Mn^{2+}, Cu^{2+}, Zn^{2+}, Mg^{2+}, Fe^{3+}, Sn^{4+}, NO_3^-, $Cr_2O_7^{2-}$, and EDTA (2 mM) were co-incubated with **DDAN** in the citric acid-phosphate buffer solution (pH 7.4), at 30 ºC for 20 min, respectively. Then, the fluorescence intensity was measured using Microplate reader (λ_{ex} 600 nm/λ_{em} 658 nm). The influences of ions on the fluorescence responses of **DDAN** towards laccase were also performed for the co-incubation of **DDAN** and laccase in the presences of various ions (2 mM). Furthermore, the various interferences of several amine acids Gln, Gly, Arg, Lys, Tyr, Trp, (1 mM) and oxidizing and reducing agents (Vitamin C, $KMnO_4$, H_2O_2, $Na_2S_2O_3$, DTT, GSH, 2 mM) were also evaluated followed the same procedures as mentioned above.

The selectivity of **DDAN** towards laccase in the presence of other biological enzymes CYP1A1, CYP2C19, CYP2D6, CYP2E1, CYP3A4, CYP3A5, Lipase, AchE, and protein BSA (1.0 mg/mL) were performed using the co-incubation of **DDAN** and these enzymes, respectively.

Sensing of fungal laccase and imaging of fungi using DDAN

All of the fungi were cultured in Yeast Extract Peptone Dextrose medium (YPD) in constant temperature shaking table (160 rpm) at 30 ºC for 12 h. The YPD medium contained yeast powder (10 g), peptone (20 g), glucose (20 g) and deionized water (1000 mL), which was sterilized at 121 ºC for 30 min. The fungal strains (24) used in the present work were standard strains, including *Aspergillus niger* AS 3.795, *Fusarium graminearum* AS 3.4598 , *Penicillium aurantiogriseum* AS 3.4512,

Aspergillus niger AS 3.1858, *Penicillium melinii* AS 3.4474, *Absidia coerulea* AS 3.3389 (**6**), *Fusarium moniliforme* AS 3.4759, *Doratomyces stemonitis* AS 3.1411, *Rhizopus stolonofer* AS 3.2050 (**9**), *Chaetomium aureum* AS 3.3783, *Alternaria alternata* AS 3.4578, *Absidia coerulea* AS 3.3538, *Chaetomium globosum* AS 3.4254, *Rhizopus oryzae* AS 3.2380, *Syncephalastrum racemosum AS 3.264*, *Sporotrichum SP. AS 3.2882*, *Cunninghamella elegans AS 3.1207*, *Mucor roxianus AS 3.3447*, *Fusarium avenaceum AS 3.4594*, *Aspergillus niger AS 3.4627*, *Mucor circinelloides AS 3.3421*, *Beauveria sp AS 3.3470*, *Alternaria longipes AS 3.2875*, *Cunninghamella echinulata AS 3.3400*. When the fungal mycelia were observed in the medium, **DDAN** was added into the medium for co-incubation at 2 h. Then, the mycelia were picked and washed by phosphate buffer, which were subjected on the slide glass for imaging measurements by Leica Confocal Microscope with the excitation wavelength at 633 nm and emission wavelength at 645 - 690 nm, respectively.

In our present work, the expression of laccase in *Aspergillus niger* and *Fusarium graminearum* were induced by 2,2'-azino-bis(3-ethylbenzothiazoline-6-sulfonic acid) (ABTS, 0.5 mM) and Cu^{2+} (0.5 mM), respectively. After the incubation of 7 days in the presences of ABTS and Cu^{2+}, respectively, the fungal laccase were imaged using **DDAN** by Confocal Microscope flowing with procedures mentioned above.

Imaging of fungal colonies on agar medium using DDAN

To investigate the capability of **DDAN** for sensing fungal laccase in different complex samples, the imaging experiment of fungal colonies has been performed in our present work. The fungal colonies of various fungi were obtained on the YPD agar medium after a culture of 2 days at 30 ºC. Under the aseptic condition, **DDAN** (50 μM) was added on the colonies drop wise for a co-incubation at 30 ºC for 2 h. Then, the plates of fungal colonies were subjected to the small animal imaging system to obtain the fluorescence images at (λ_{ex} 630 nm/λ_{em} 665 – 735 nm).

Activity assay of fungal laccase in the fungal lysates

The fungi were cultured in YPD medium for 3 days to afford the mycelia. 200 mg mycelia were suspended in 6 mL PBS and broke on the ice using high speed tissue homogenizer (10 second each time for 5 times, with the interval of 30 second). Then,

the suspension solutions were centrifuged at 4 ºC and 6000 rpm for 20 min, which would give the fungal lysates containing laccase.

Assay of the laccase activity about the fungal lysates were performed using **DDAN**. The co-incubation of lysates and **DDAN** (10 μM) were conducted at 30 ˚C for 20 min. After the enzymatic reaction was terminated by acetonitrile (33%, *v/v*), the fluorescence intensity of solution was recorded by microplate reader (λ_{ex} 600 nm/λ_{em} 658 nm).

The synthesis of dicoumarin mediated by fungal laccase

10 g mycelia of fungus *Rhizopus oryzae* AS 3.2380 were broken to give fungal lysates. The co-incubation of 6,7-dihydroxycoumarin (100 mg) and fungal lysates in PBS for 1h was performed and extracted by ethyl acetate. The extract was separated by preparative HPLC and the oxidation product dicoumarin was obtained. The structure of dicoumarin was determined by ^{1}H, ^{13}C NMR, HSQC, HMBC, ESI-MS, and HRESI-MS. UV (CH_3OH) λ_{max} 346.5 nm; ^{1}H NMR (DMSO-d_6, 500 MHz) δ_H 6.07 (d, J = 9.5 Hz, H-3), 7.15 (d, J = 9.5 Hz, H-4), 6.16 (d, J = 9.0 Hz, H-3'), 7.96 (d, J = 9.0 Hz, H-4'), δ_H 6.88 (s, H-8), 7.12 (brs, H-5'). ^{13}C NMR (DMSO-d_6, 125 MHz) δ_C 160.5 (C-2), 111.4 (C-3), 142.7 (C-4), 116.3 (C-5), 141.2 (C-6), 150.1 (C-7), 101.9 (C-8), 148.5 (C-9), 110.2 (C-10), 160.7 (C-2'), 111.4 (C-3'), 144.7 (C-4'), 111.7 (C-5'), 142.3 (C-6'), 148.6 (C-7'), 109.2 (C-8'), 146.8 (C-9'), 110.6 (C-10'); HRESI-MS *m/z* 353.0299 $[M-H]^-$ (calcd for $C_{18}H_9O_8$, 353.0927).

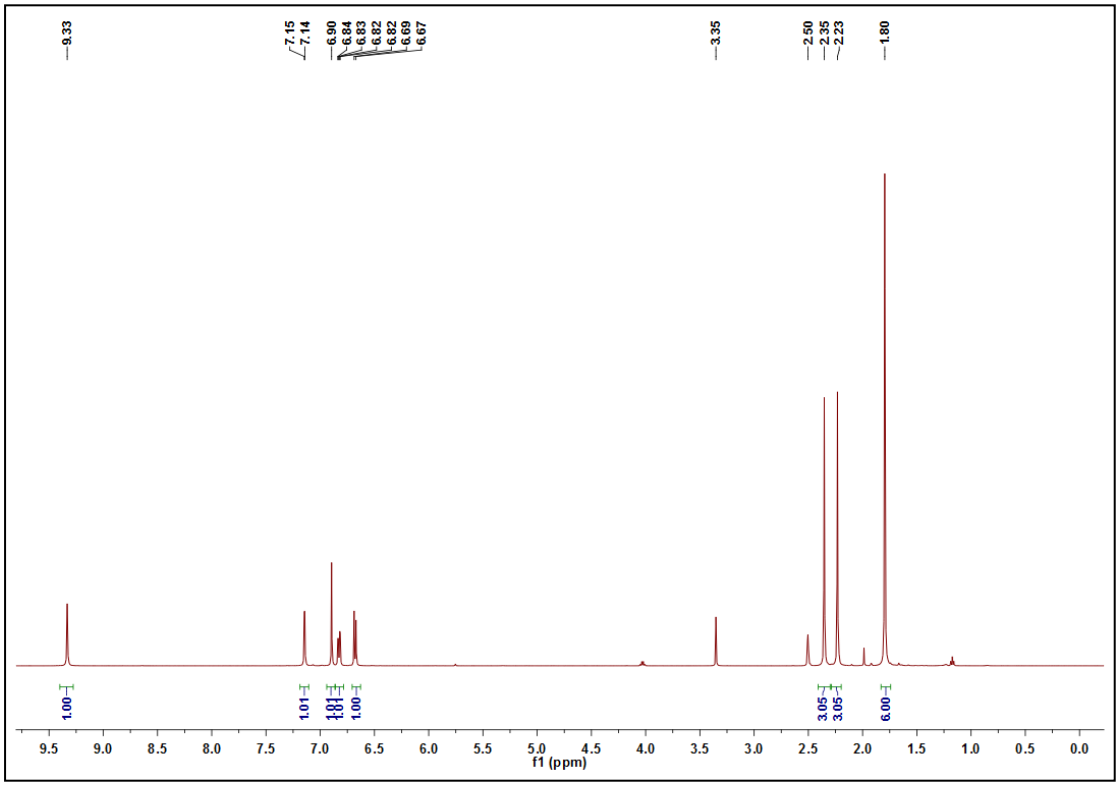

Fig. S1. ^{1}H NMR spectrum of **4**.

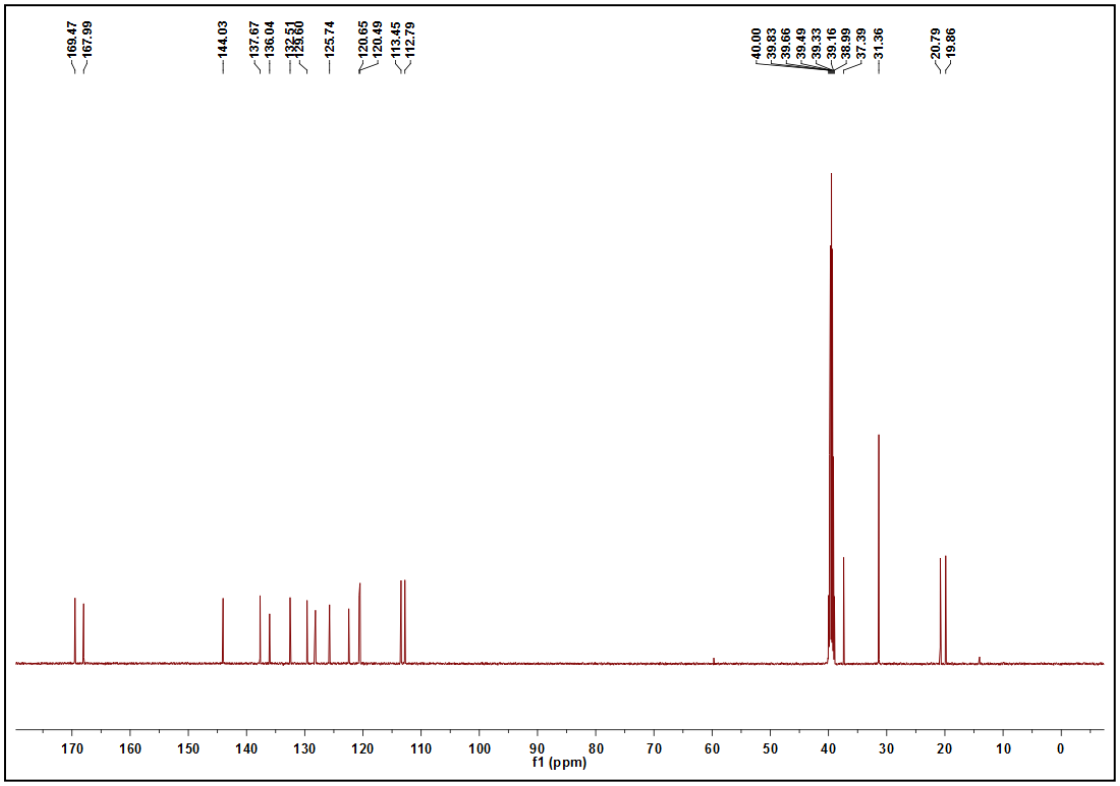

Fig. S2. ^{13}C NMR spectrum of **4**.

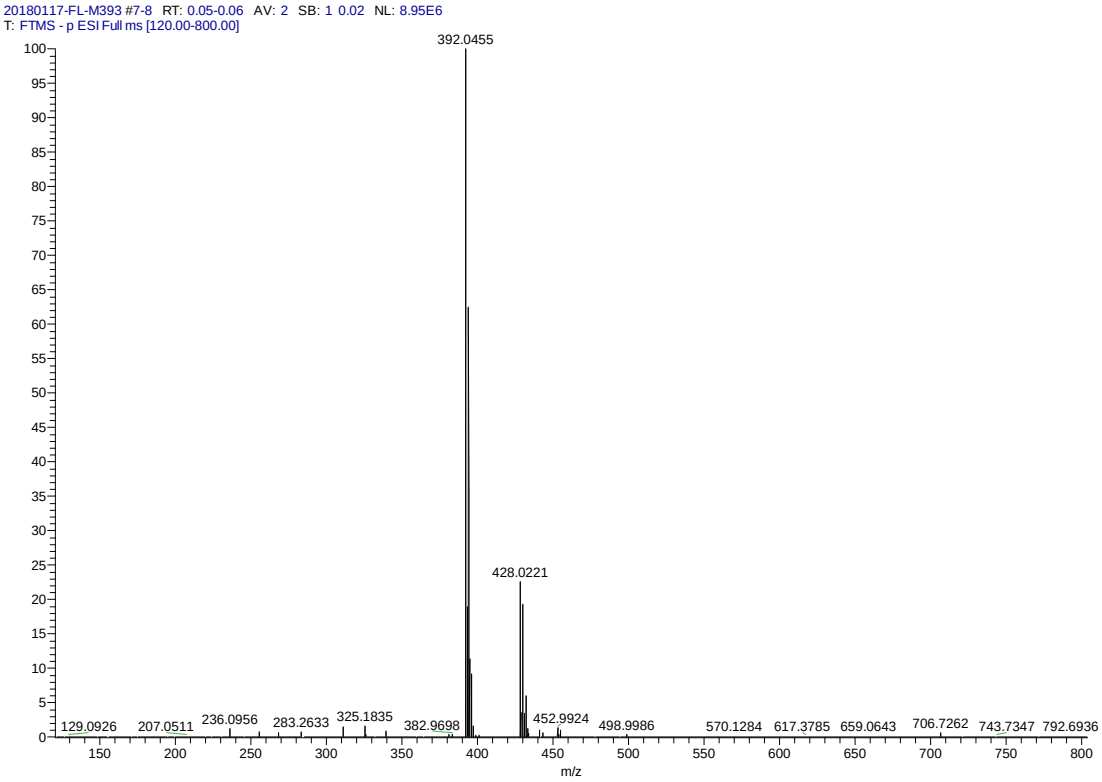

Fig. S3. HR-MS spectrum of **4**.

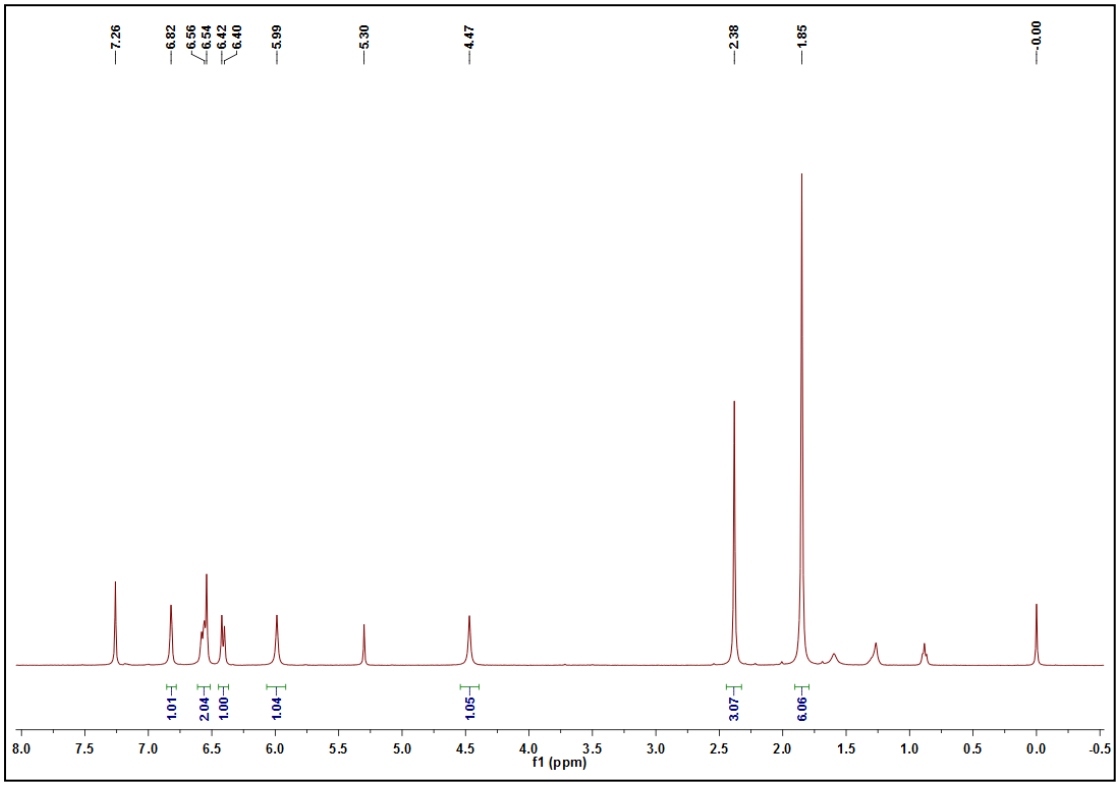

Fig. S4. ^{1}H NMR spectrum of **DDAN**.

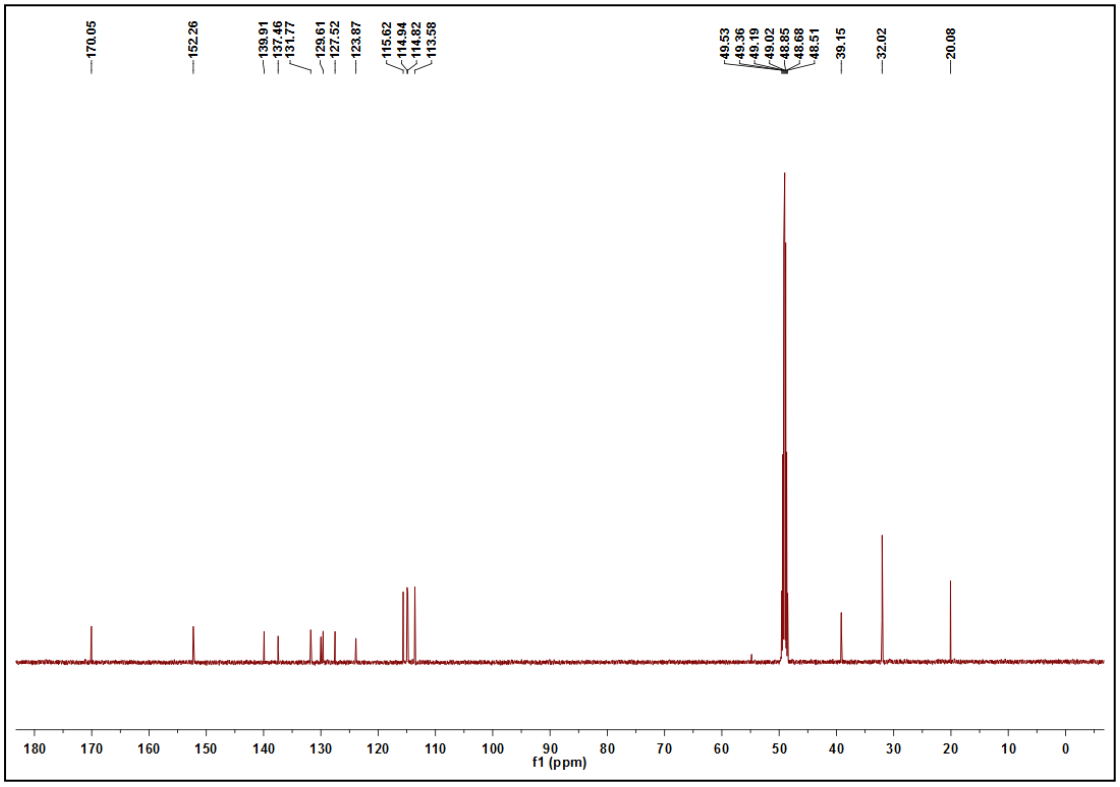

Fig. S5. ^{13}C NMR spectrum of **DDAN**.

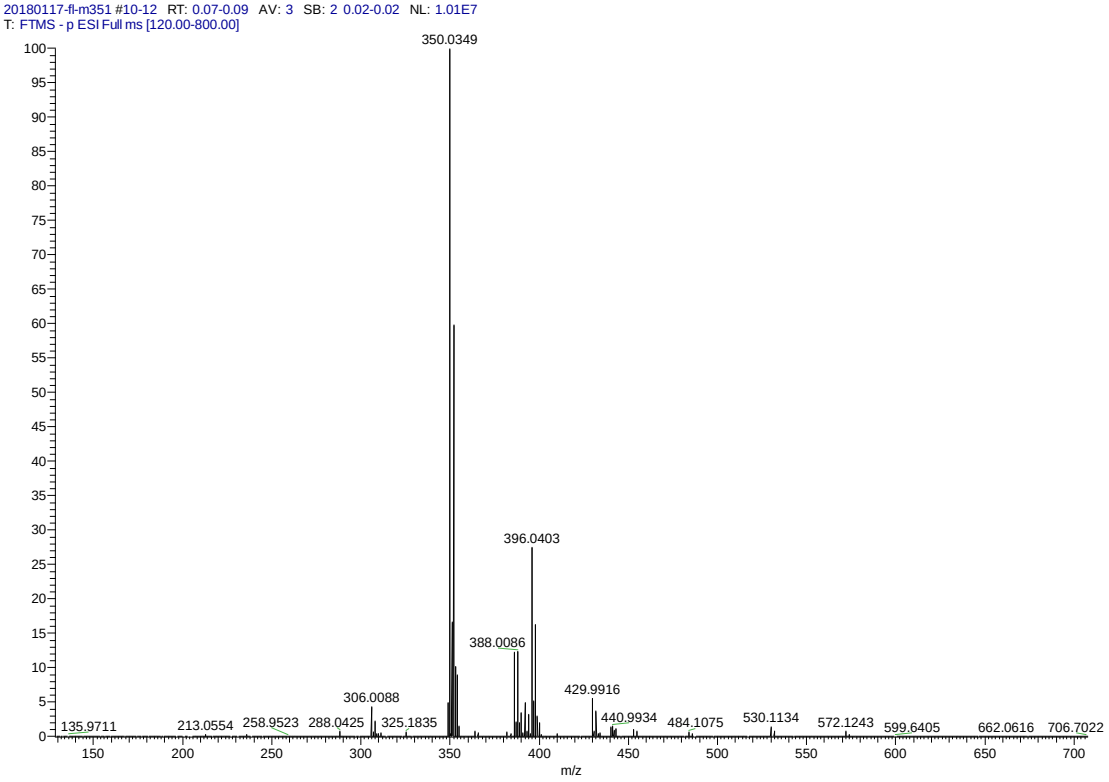

Fig. S6. HR-MS spectrum of **DDAN**.

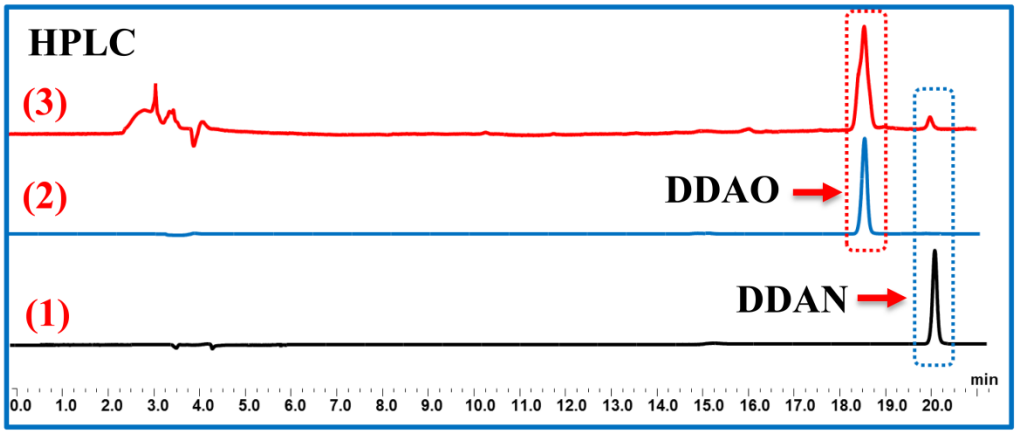

Fig. S7. HPLC chromatograms for the enzymatic reaction about **DDAN** mediated by laccase (1. standard **DDAN**; 2. standard **DDAO**; 3. co-incubation of **DDAN** and laccase)

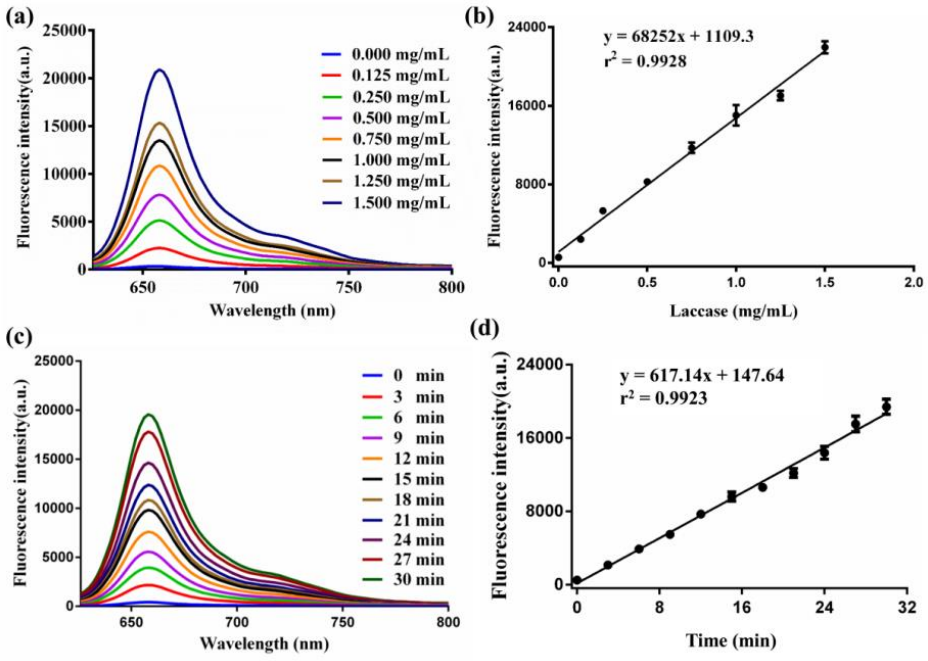

Fig. S8. (a) Fluorescence spectra of **DDAN** (10 μM) upon the addition of increasing concentrations of laccase (0 – 1.5 mg/mL) with the incubation of 20 min. (b) Fluorescence intensity of **DDAN** upon the addition of increasing concentrations of laccase (0 – 1.5 mg/mL) with the incubation of 20 min. (c) Fluorescence spectra recorded following co-incubation of **DDAN** (10 μM) towards laccase (1.0 mg/mL) at various incubation time points. (d) The plot of fluorescence intensity at 658 nm versus reaction time. The enzymatic reactions were performed in phosphate citric acid buffer (pH 7.4) at 30 °C for 20 min, and terminated by acetonitrile (50%, *v/v*). Then, the fluorescence emission was measured in citric acid-phosphate buffer: acetonitrile (*v/v* = 1:1), λ_{ex} = 600 nm; λ_{em} = 658 nm.

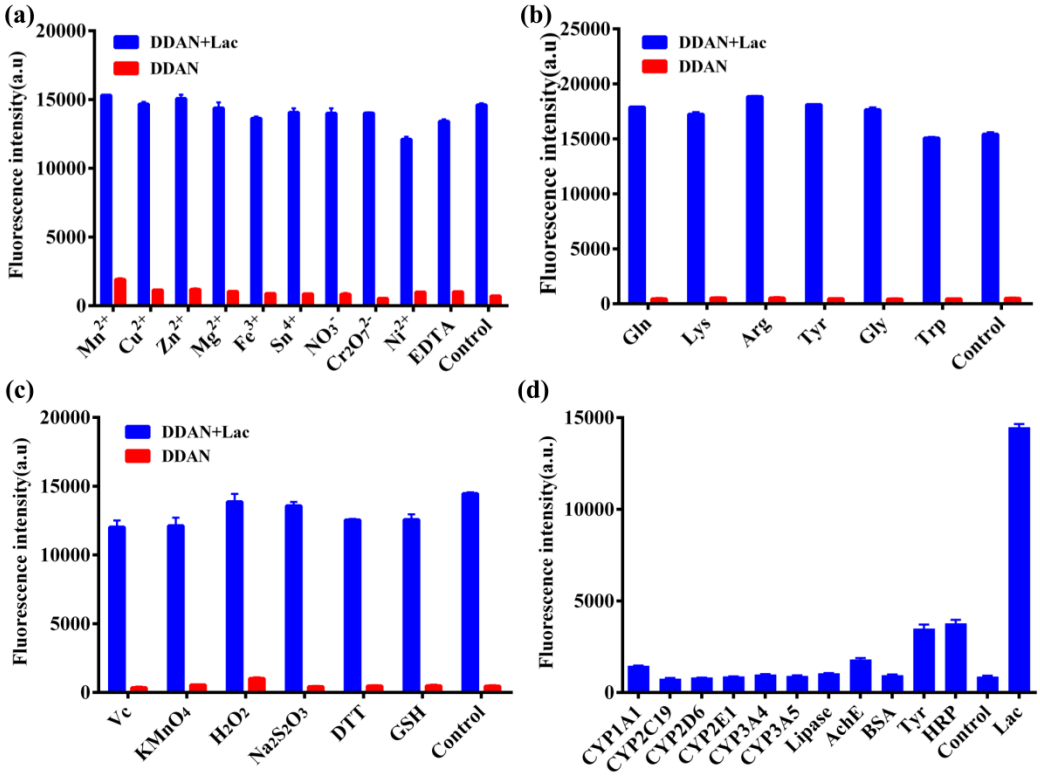

Fig. S9. The interferences of various species on the fluorescence intensity of **DDAN** and the enzymatic system for the co-incubation of **DDAN** and laccase (Lac). (a) Interferences of various ions: Mn^{2+}, Cu^{2+}, Zn^{2+}, Mg^{2+}, Fe^{3+}, Sn^{4+}, NO_3^-, $Cr_2O_7^{2-}$, and EDTA (2 mM). (b) Interferences of several amine acids (Gln, Gly, Arg, Lys, Tyr, Trp, 1 mM). (c) Interferences of several oxidizing and reducing agents (Vitamin C, $KMnO_4$, H_2O_2, $Na_2S_2O_3$, DTT, GSH, 2 mM). (d) Selectivity of **DDAN** towards laccase in the presence of other biological enzymes and proteins (1.0 mg/mL). (λ_{ex} = 600 nm; λ_{em} = 658 nm)

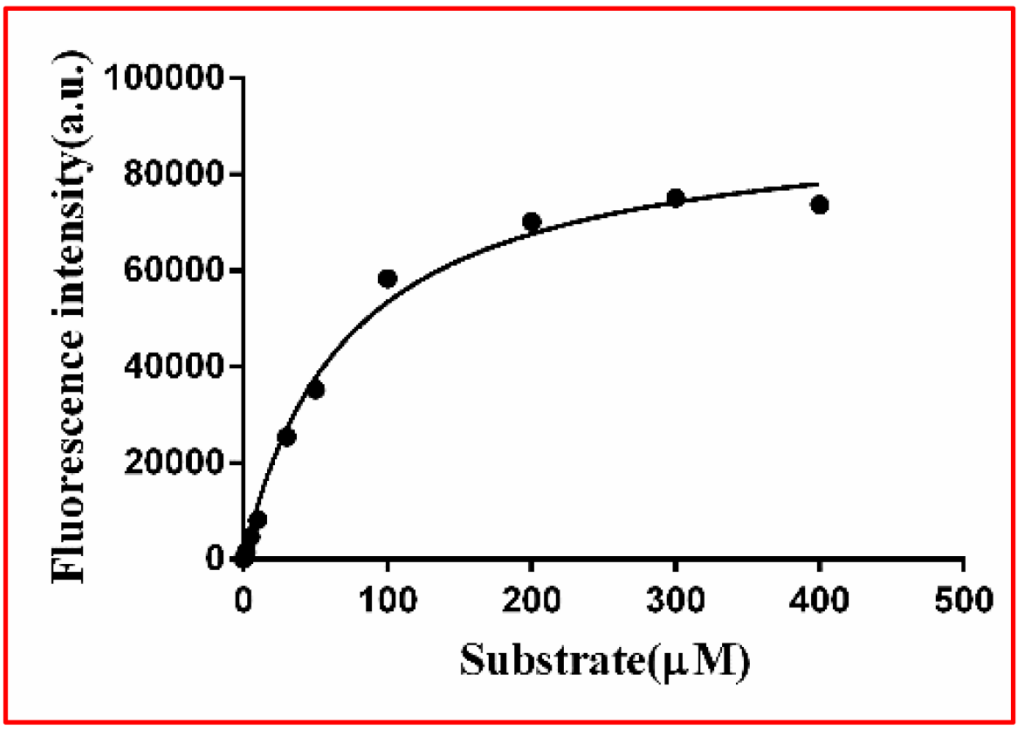

Fig. S10. The kinetics of the oxidation of **DDAN** mediated by laccase. (λ_{ex} = 600 nm; λ_{em} = 658 nm.

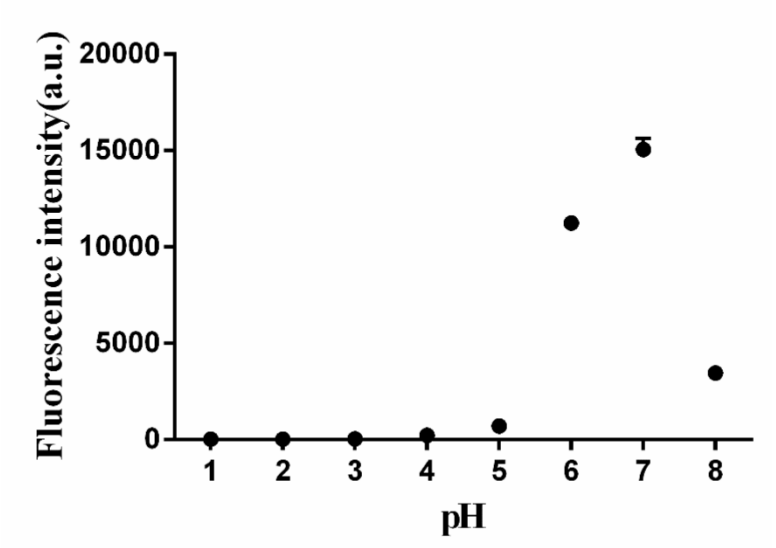

Fig. S11. The interference of pH values about the enzymatic solution for the fluorescence intensity of **DDAN** towards laccase.

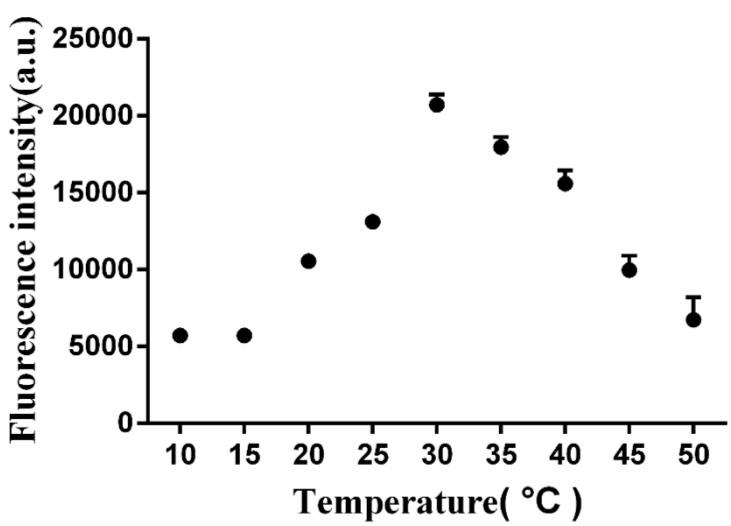

Fig. S12. The influence of incubation temperature for the intensity of **DDAN** towards laccase.

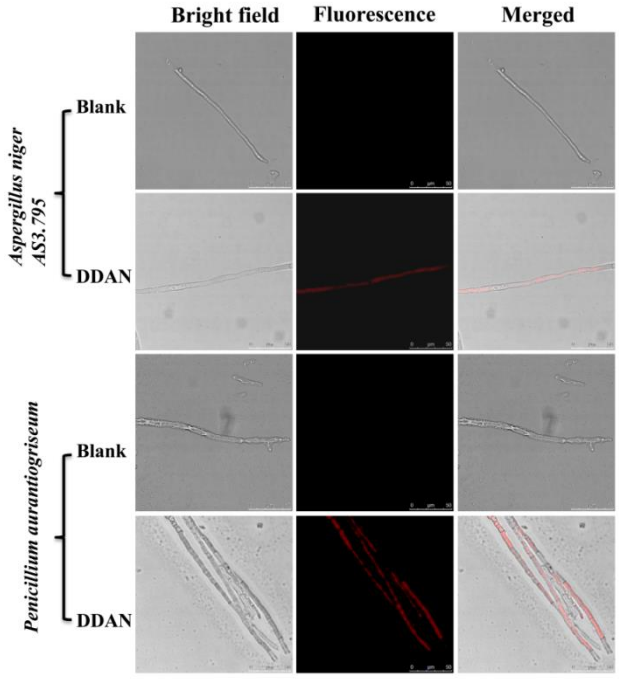

Fig. S13. Confocal laser scanning microscopy (CLSM) images of fungal mycelia in the presence of **DDAN** (50 μM). *Aspergillus niger AS 3.795* and *Penicillium aurantiogriseum AS 3.4512*. Excitation, 633 nm; Emission, 645−690 nm. Scale bar: 50 μm.

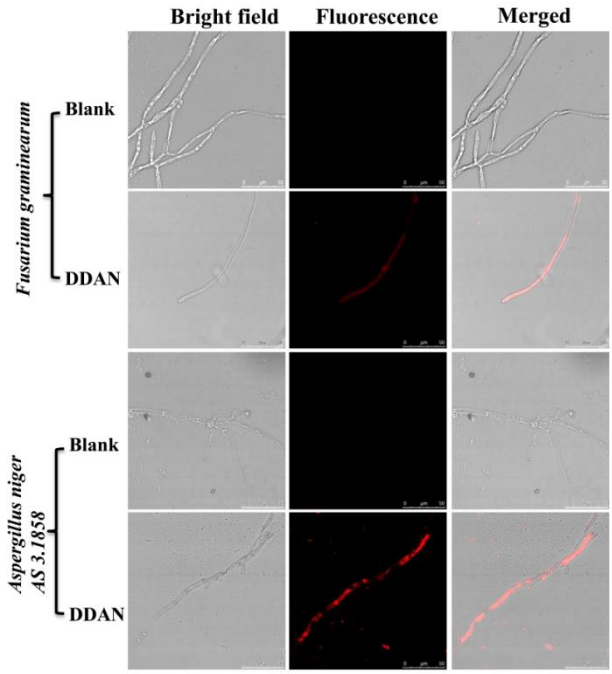

Fig. S14. Confocal laser scanning microscopy (CLSM) images of fungal mycelia in the presence of **DDAN** (50 μM). *Fusarium graminearum AS 3.4598* and *Alternaria alternate AS 3.1858*. Excitation, 633 nm; Emission, 645−690 nm. Scale bar: 50 μm.

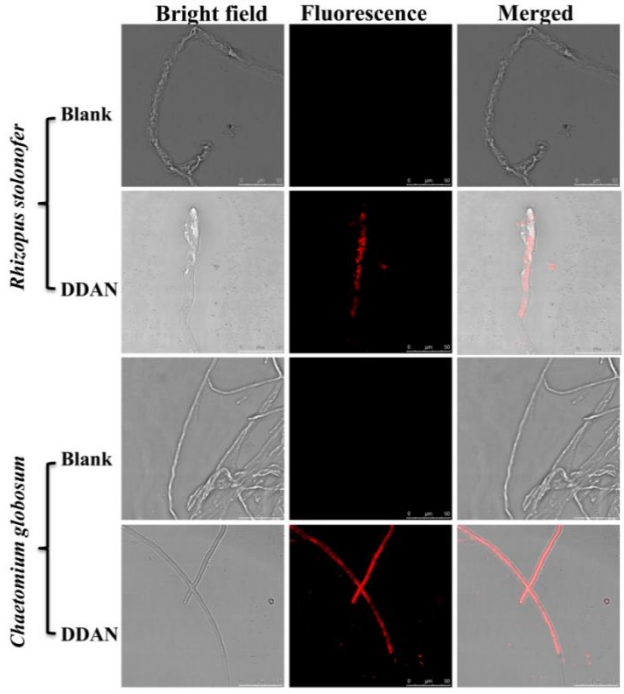

Fig. S15. Confocal laser scanning microscopy (CLSM) images of fungal mycelia in the presence of **DDAN** (50 μM). *Rhizopus stolonofer AS 3.2050* and *Chaetomium globosum AS 3.4254*. Excitation, 633 nm; Emission, 645−690 nm. Scale bar: 50 μm.

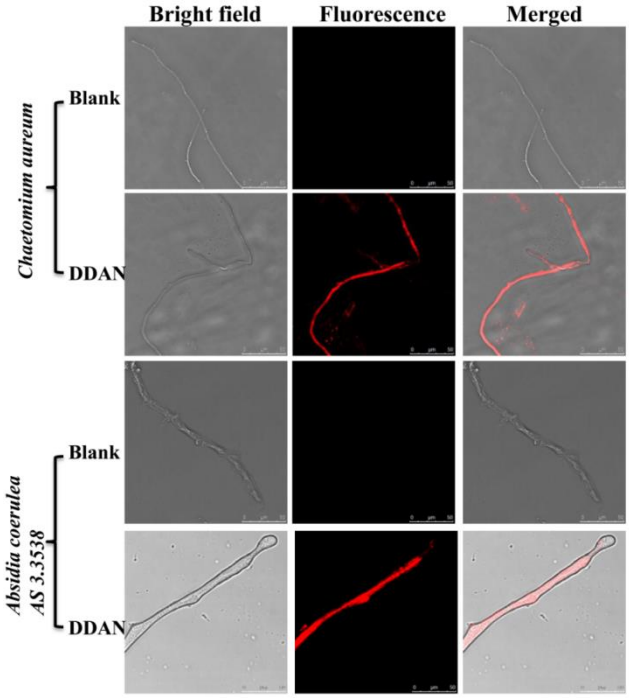

Fig. S16. Confocal laser scanning microscopy (CLSM) images of fungal mycelia in the presence of **DDAN** (50 μM). *Chaetomium aureum AS 3.3783* and *Absidia coerulea AS 3.3538*. Excitation, 633 nm; Emission, 645−690 nm. Scale bar: 50 μm.

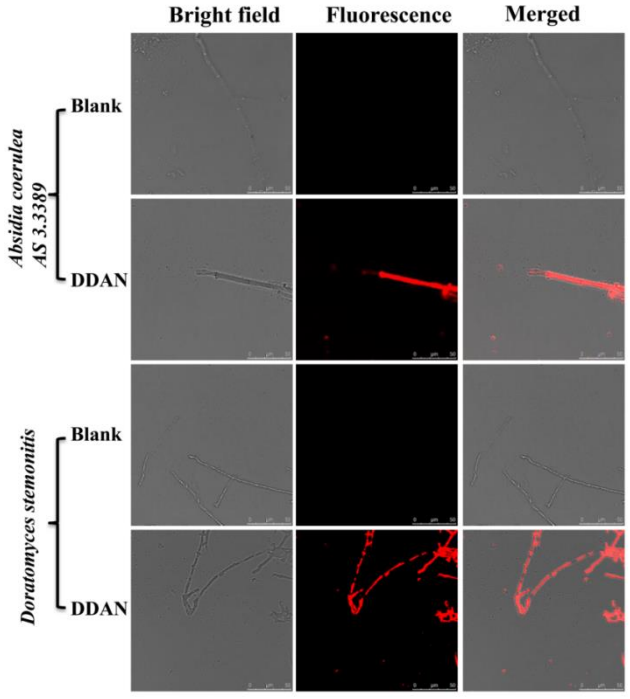

Fig. S17. Confocal laser scanning microscopy (CLSM) images of fungal mycelia in the presence of **DDAN** (50 μM). *Absidia coerulea AS 3.3389* and *Doratomyces stemonitis AS 3.1411*. Excitation, 633 nm; Emission, 645−690 nm. Scale bar: 50 μm.

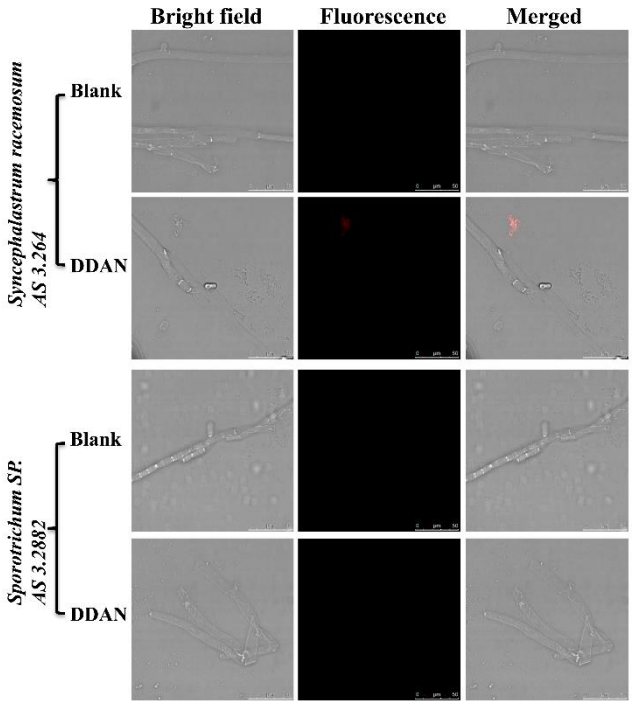

Fig. S18. Confocal laser scanning microscopy (CLSM) images of fungal mycelia in the presence of **DDAN** (50 μM). *Syncephalastrum racemosum AS 3.264* and *Sporotrichum SP. AS 3.2882*. Excitation, 633 nm; Emission, 645−690 nm. Scale bar: 50 μm.

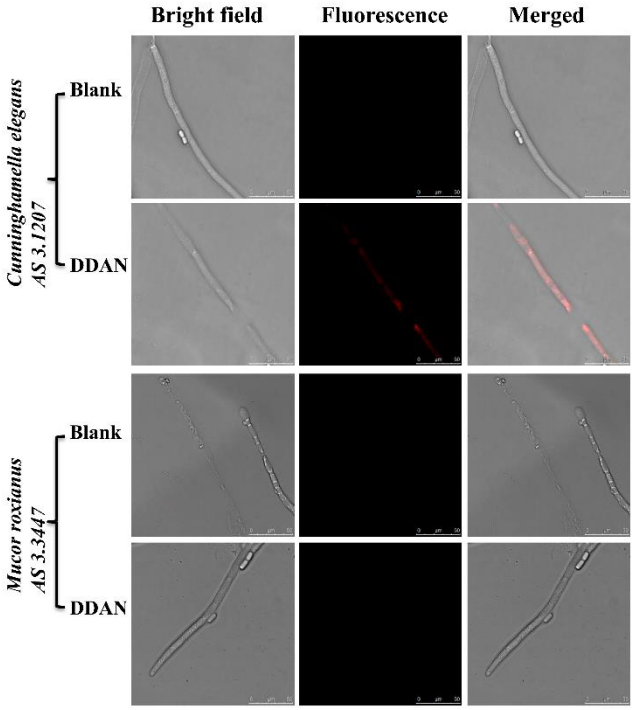

Fig. S19. Confocal laser scanning microscopy (CLSM) images of fungal mycelia in the presence of **DDAN** (50 μM). *Cunninghamella elegans AS 3.1207* and *Mucor roxianus AS 3.3447*. Excitation, 633 nm; Emission, 645−690 nm. Scale bar: 50 μm.

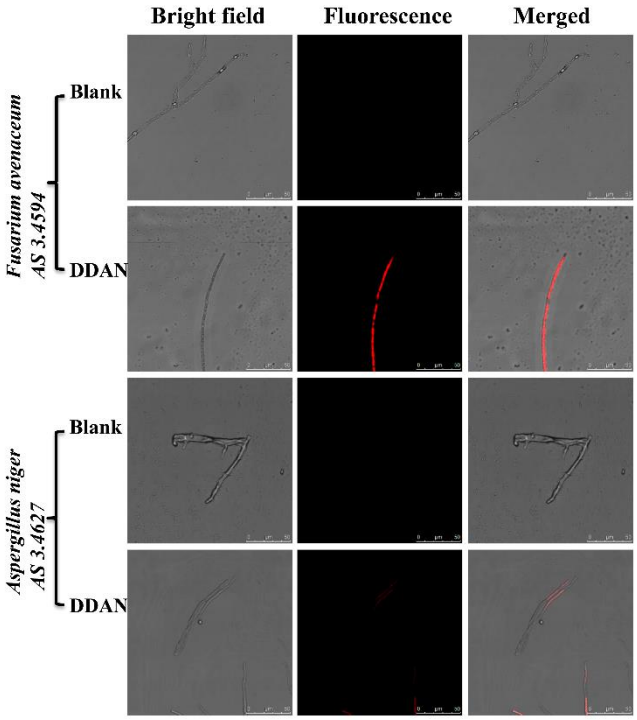

Fig. S20. Confocal laser scanning microscopy (CLSM) images of fungal mycelia in the presence of **DDAN** (50 μM). *Fusarium avenaceum AS 3.4594* and *Aspergillus niger AS 3.4627*. Excitation, 633 nm; Emission, 645−690 nm. Scale bar: 50 μm.

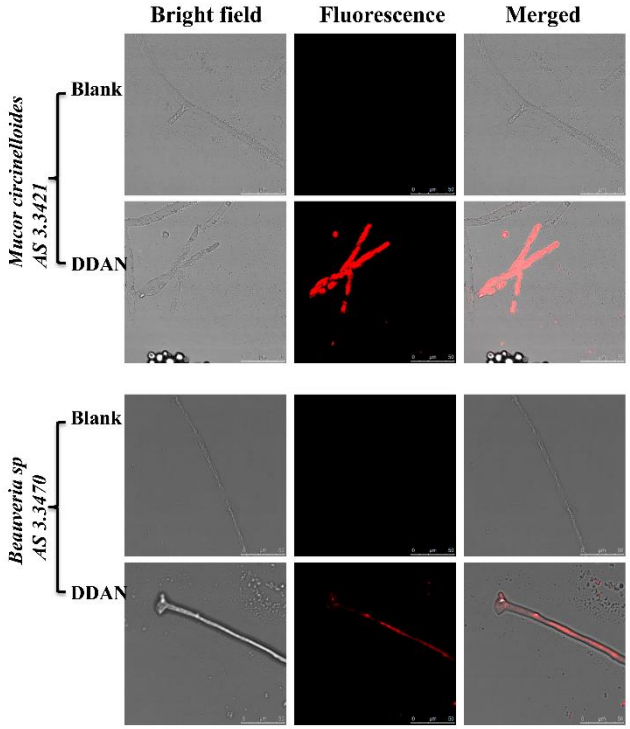

Fig. S21. Confocal laser scanning microscopy (CLSM) images of fungal mycelia in the presence of **DDAN** (50 μM). *Mucor circinelloides AS 3.3421* and *Beauveria sp AS 3.3470*. Excitation, 633 nm; Emission, 645−690 nm. Scale bar: 50 μm.

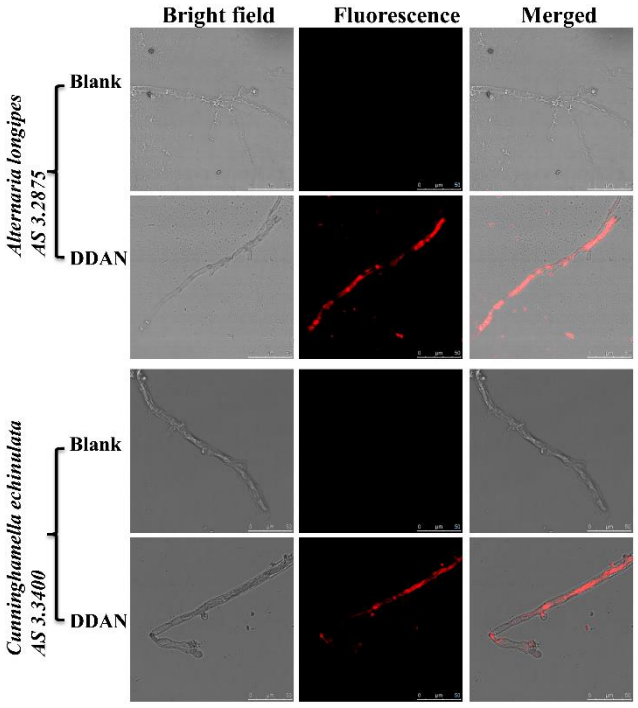

Fig. S22. Confocal laser scanning microscopy (CLSM) images of fungal mycelia in the presence of **DDAN** (50 μM). *Alternaria longipes AS 3.2875* and *Cunninghamella echinulata AS 3.3400*. Excitation, 633 nm; Emission, 645−690 nm. Scale bar: 50 μm.

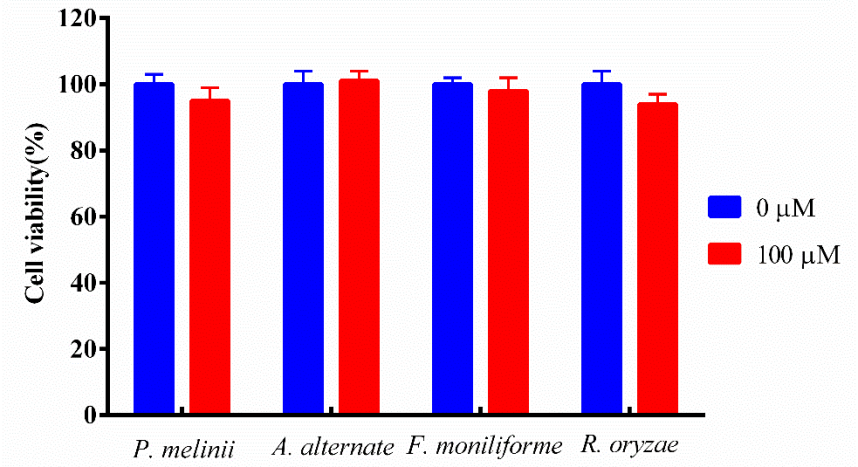

Fig. S23. The cytotoxic activity of **DDAN** on fugal cells (*Penicillium melinii AS 3.4474*, *Alternaria alternate AS 3.4578*, *Fusarium moniliforme AS 3.4759*, and *Rhizopus oryzae AS 3.2380*) at 100 μM.

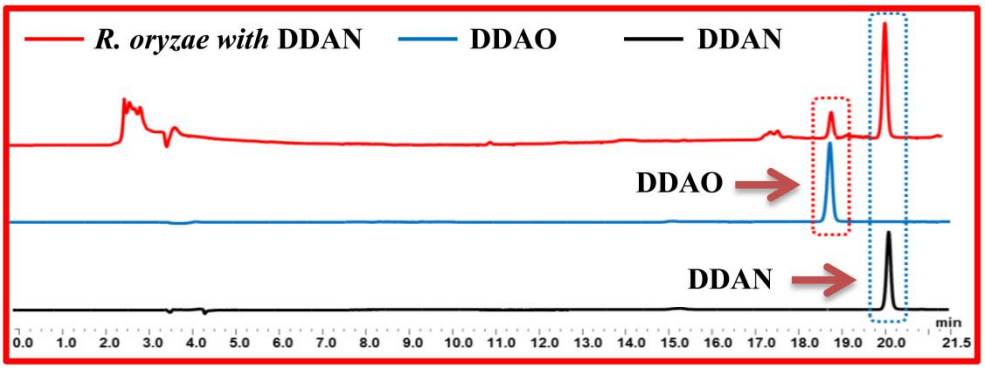

Fig. S24. HPLC chromatograms for the oxidation of **DDAN** mediated by *R. oryzae*.

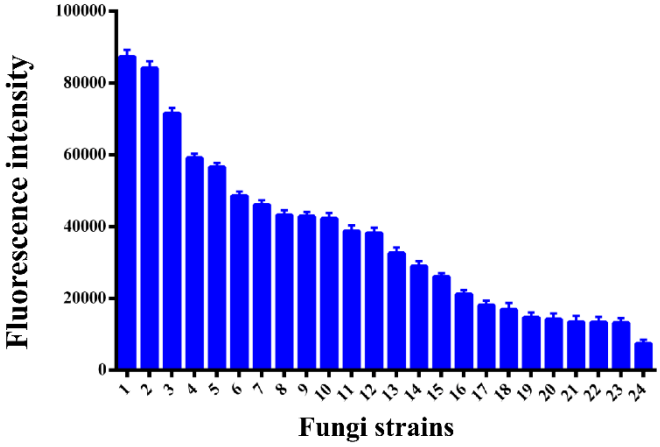

Fig. S25. The activity assay of endogenous laccase about 24 fungi strains using the fluorescent probe **DDAN**. (λ_{ex} = 600 nm; λ_{em} = 658 nm) *Rhizopus oryzae* AS 3.2380 (1), *Fusarium moniliforme AS 3.4659* (2), *Alternaria alternate AS 3.4578* (3), *Penicillium melinii AS 3.4474* (4), *Penicillium aurantiogriseum AS 3.4512* (5), *Mucor circinelloides AS 3.3421* (6), *Alternaria longipes AS 3.2875* (7), *Cunninghamella echinulata AS 3.3400* (8), *Absidia coerulea AS 3.3389* (9), *Doratomyces stemonitis AS 3.1411* (10), *Fusarium avenaceum AS 3.4594* (11), *Aspergillus niger AS 3.4627* (12), *Fusarium graminearum AS 3.4598* (13), *Alternaria alternate AS 3.1858* (14), *Rhizopus stolonofer AS 3.2050* (15), *Chaetomium globosum AS 3.4254* (16), *Chaetomium aureum AS 3.3783* (17), *Absidia coerulea AS 3.3538* (18), *Beauveria sp AS 3.3470* (19), *Aspergillus niger AS 3.795* (20), *Cunninghamella elegans AS 3.1207* (21), *Mucor roxianus AS 3.3447* (22), *Syncephalastrum racemosum AS 3.264* (23), *Sporotrichum SP. AS 3.2882* (24).

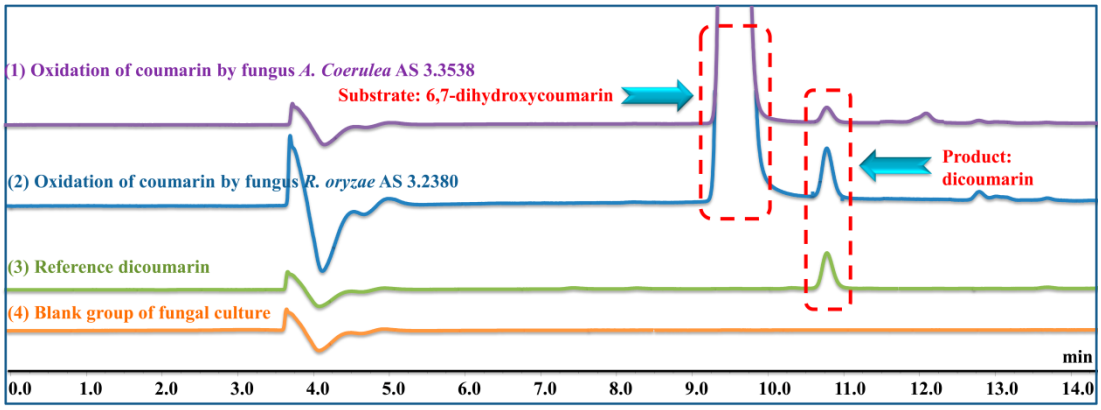

Fig. S26. HPLC chromatograms for the oxidation of 6,7-dihydroxycoumarin mediated by fungus *Rhizopus oryzae* AS 3.2380.

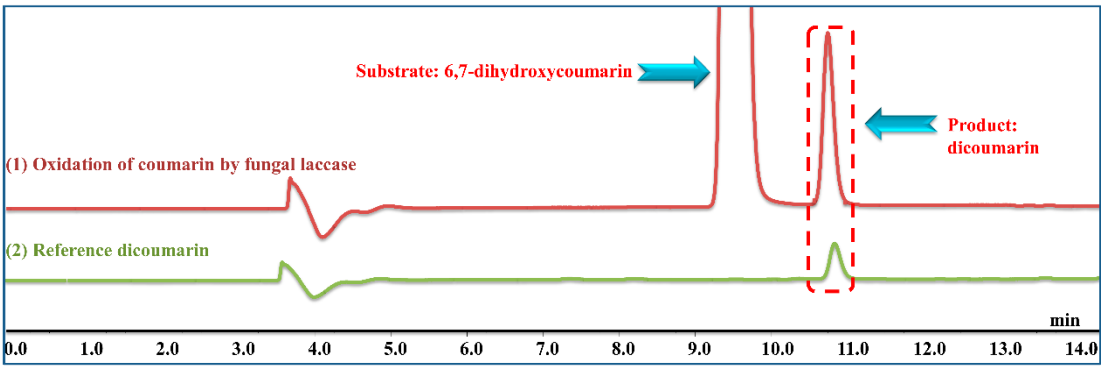

Fig. S27. HPLC chromatograms for the oxidation of 6,7-dihydroxycoumarin mediated by fungal laccase.

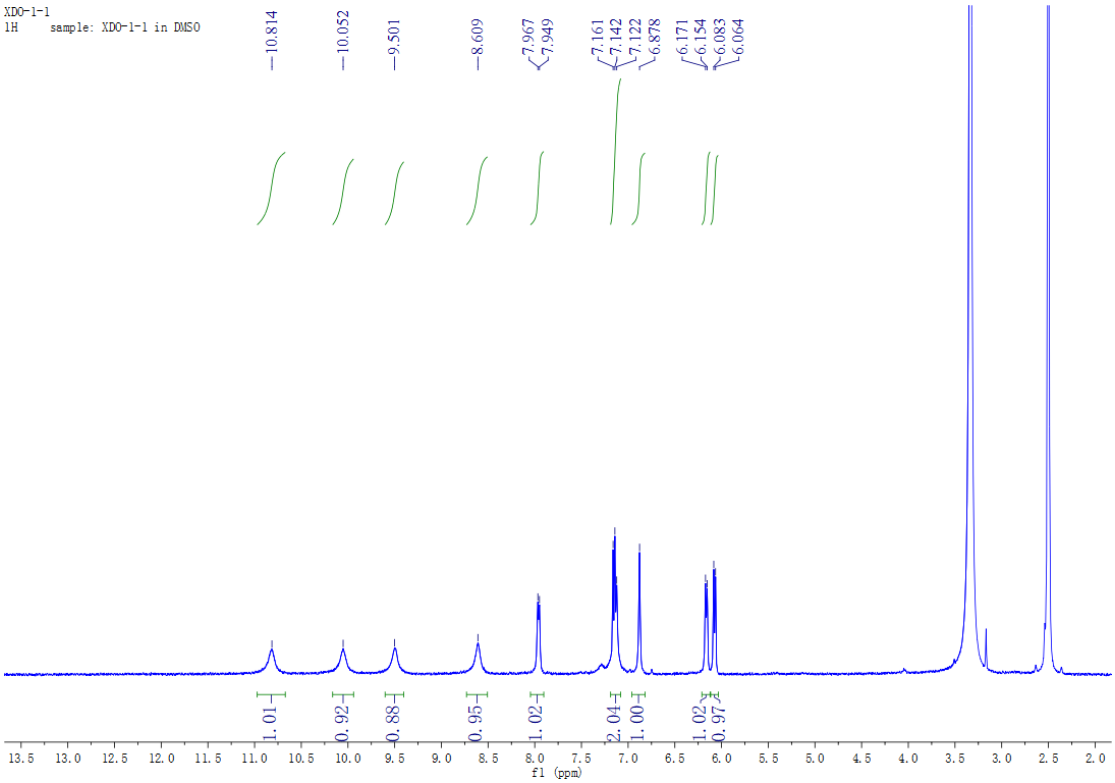

Fig. S28. ^{1}H NMR (DMSO-d_6, 600 MHz) spectrum of 6,6',7,7'-tetrahydroxy-2H,2'H-(5,8'- bichromene)-2,2'-dione.

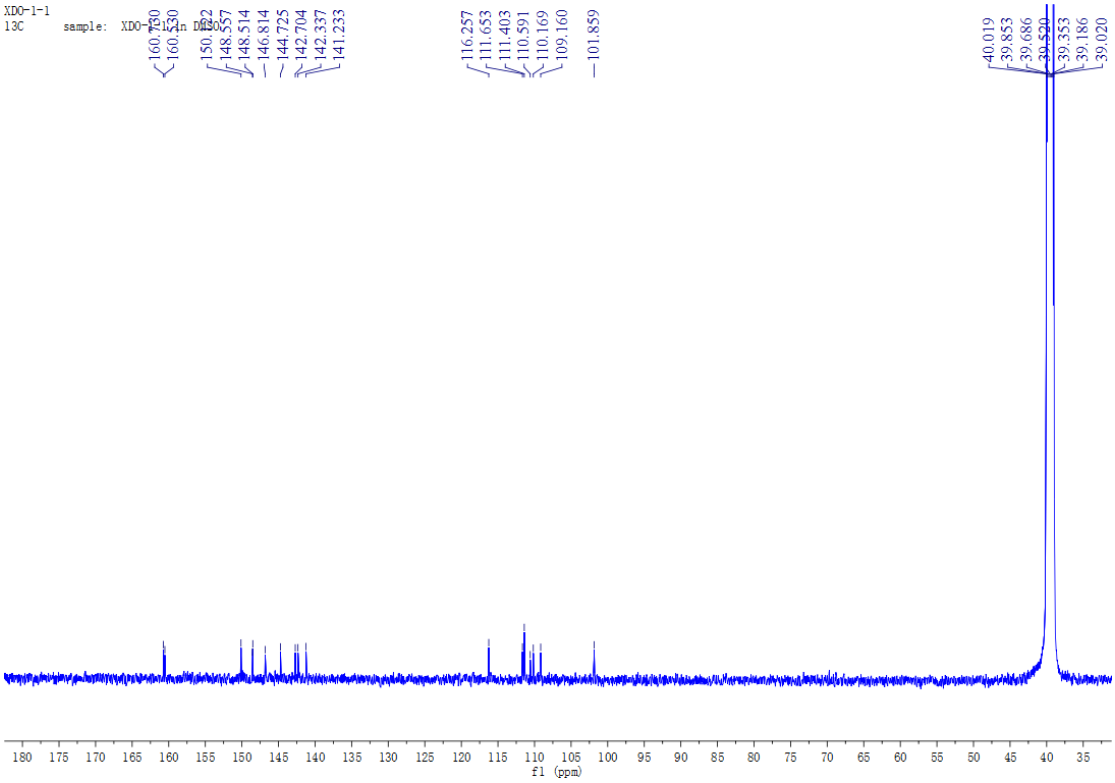

Fig. S29. ^{13}C NMR (DMSO-d_6, 150 MHz) spectrum of 6,6',7,7'-tetrahydroxy-2H,2'H-(5,8'- bichromene)-2,2'-dione.

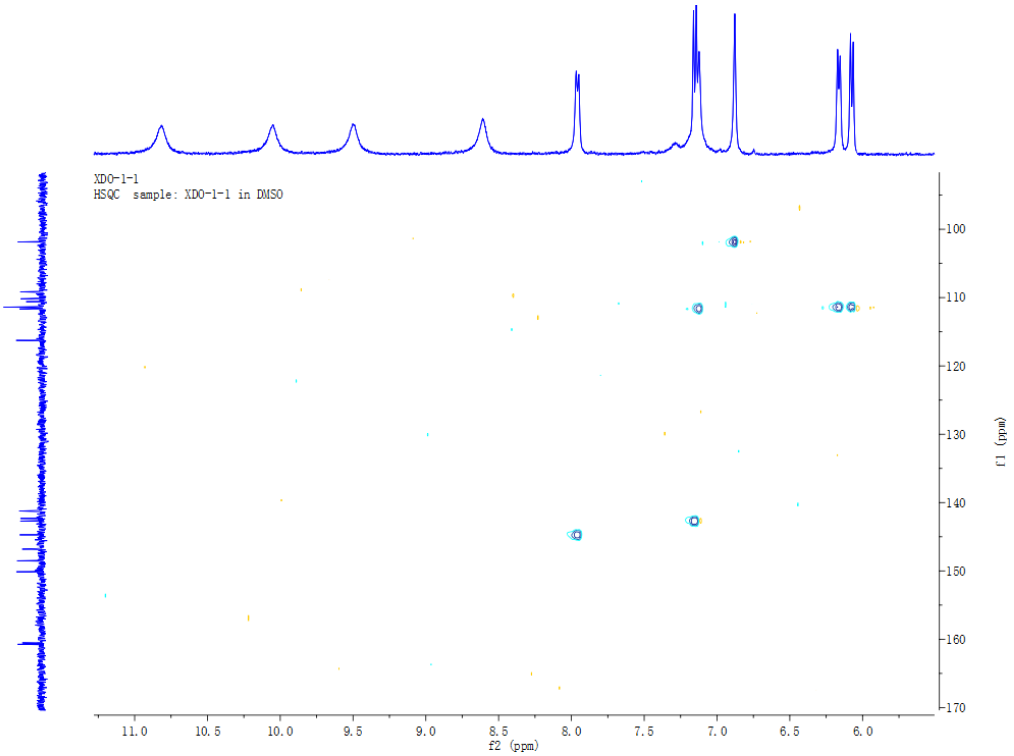

Fig. S30. HSQC spectrum of 6,6',7,7'-tetrahydroxy-2H,2'H-(5,8'- bichromene)-2,2'-dione.

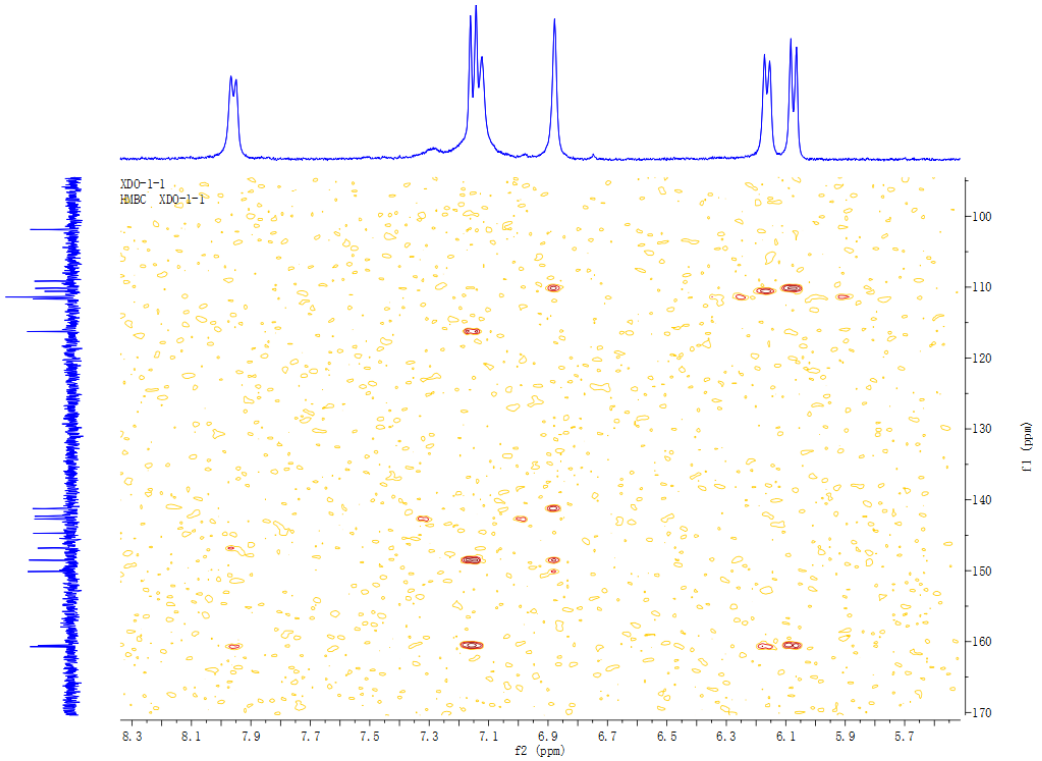

Fig. S31. HMBC spectrum of 6,6',7,7'-tetrahydroxy-2H,2'H-(5,8'- bichromene)-2,2'-dione.

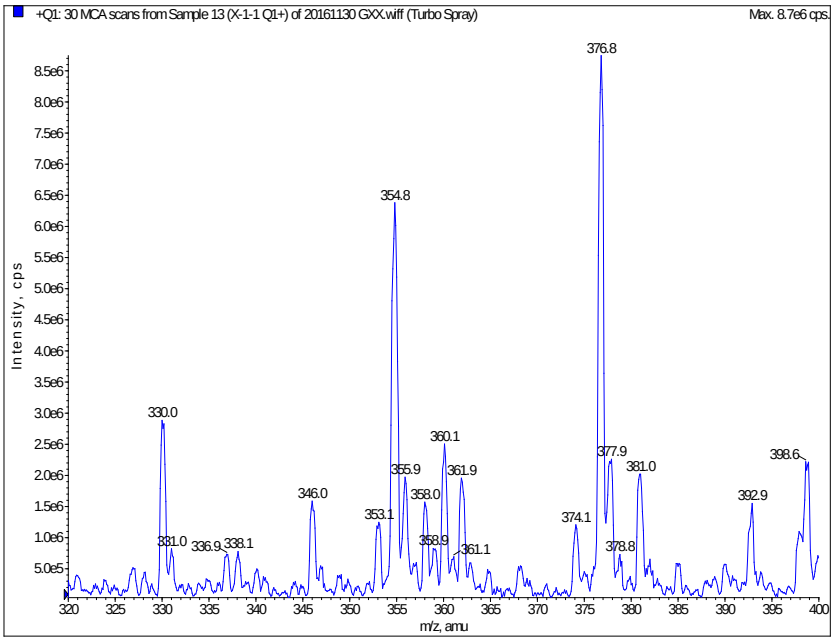

Fig. S32. (+)-ESI-MS spectrum of 6,6',7,7'-tetrahydroxy-2H,2'H-(5,8'- bichromene)-2,2'-dione.

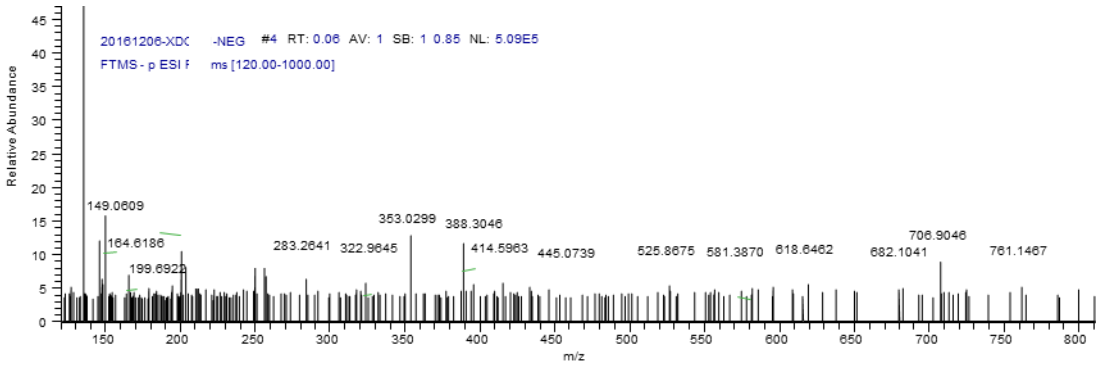

Fig. S33. (-)-HRESI-MS spectrum of 6,6',7,7'-tetrahydroxy-2H,2'H-(5,8'-bichromene)-2,2'-dione.

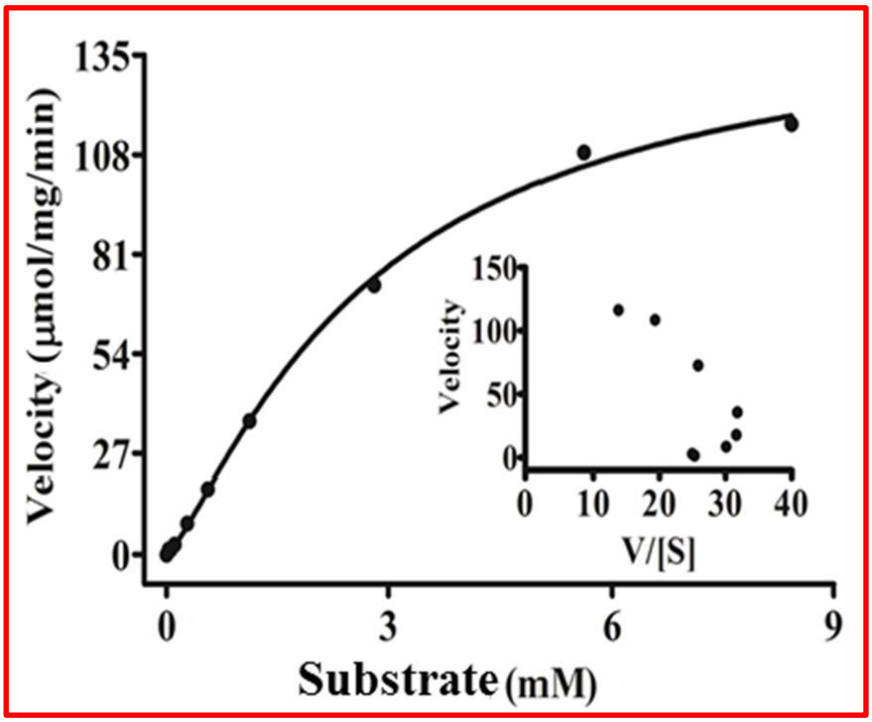

Fig. S34. The kinetics profile for the biosynthesis of dicoumarin.

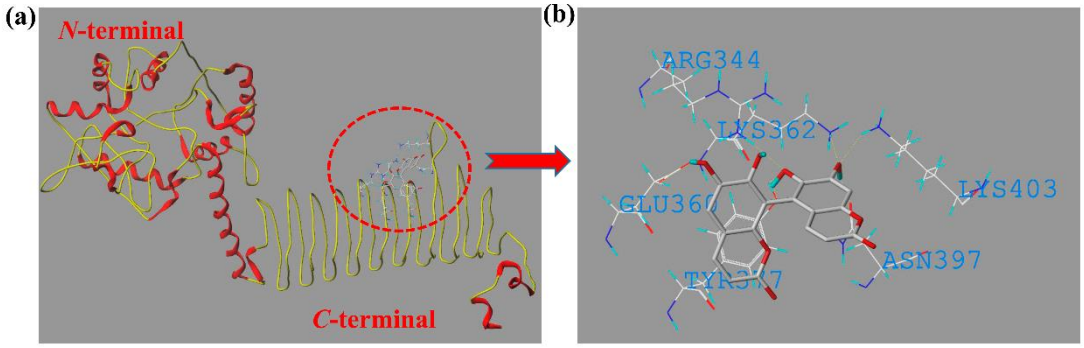

Fig. S35. In silico docking analysis between dicoumarin 6,6',7,7'-tetrahydroxy-2H,2'H-(5,8'- bichromene)-2,2'-dione and GlmU protein (PDB No. 4k6r).